Supplemental Figures

Mapping Sentinel Lymph Node Metastasis by Dual-Probe Optical Imaging

Xiangyu Yang[1,2], Zhe Wang[2], Fuwu Zhang[2], Guizhi Zhu[2], Jibin Song[2], Gao-Jun Teng[1*], Gang Niu[2*], Xiaoyuan Chen[2*]

Table of Contents

Supplemental Figure 1. Cytotoxicity of Cy5.5-HA.

Supplemental Figure 2. Fluorescence imaging of inflamed lymph nodes with Cy5.5-HA10K.

Supplemental Figure 3. Sensitivity assay of IRDye800-cetuximab in detecting UM-SCC-22B tumor cells in vivo.

Supplemental Figure 4. Development and monitoring of UM-SCC-22B metastasis model.

Supplemental Figure 5. Development and monitoring of SKOV-3 metastasis model.

Supplemental Figure 6. Separation of fluorescence signals from Cy5.5-HA10 and IRDye800-mAb.

Supplemental Figure 7. Mapping tumor metastasis in sentinel lymph nodes by dual-probe fluorescence optical imaging in SKOV-3 metastasis model.

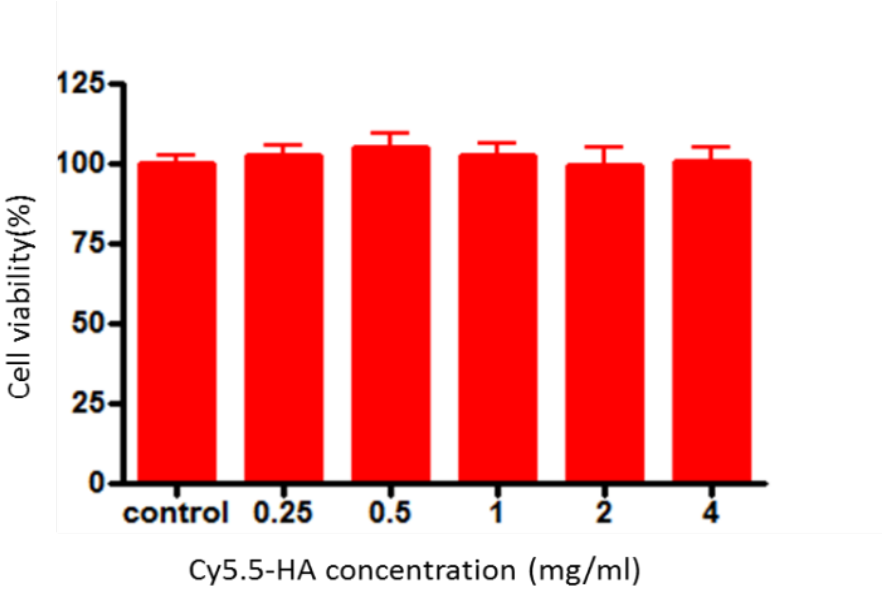

Supplemental Figure 1. Cytotoxicity of Cy5.5-HA. The toxicity of Cy5.5-HA to UM-SCC-22B cells was determined by MTT assay. All studies were performed with triplicate samples and repeated at least three times. Briefly, cells were harvested by trypsinization, resuspended in DMEM medium, and plated in a 96-well plate at 2000 cells per well. At 72 h after treatment with different doses of Cy5.5-HA (ranging from 0.25 to 4 mg/ml), the culture medium was replaced and 50 μL of 1.0 mg/ml sterile filtered 3-(4, 5-dimethylthiazol-2-yl)-2, 5-diphenyl tetrazolium bromide (MTT; Sigma) was added to each well. The unreacted dye was removed after 4 h and the insoluble formazan crystals were dissolved in 150 μL of DMSO. The absorbance at 570 nm (reference wavelength: 630 nm) was measured with a microplate reader (Synergy 2, BioTek).

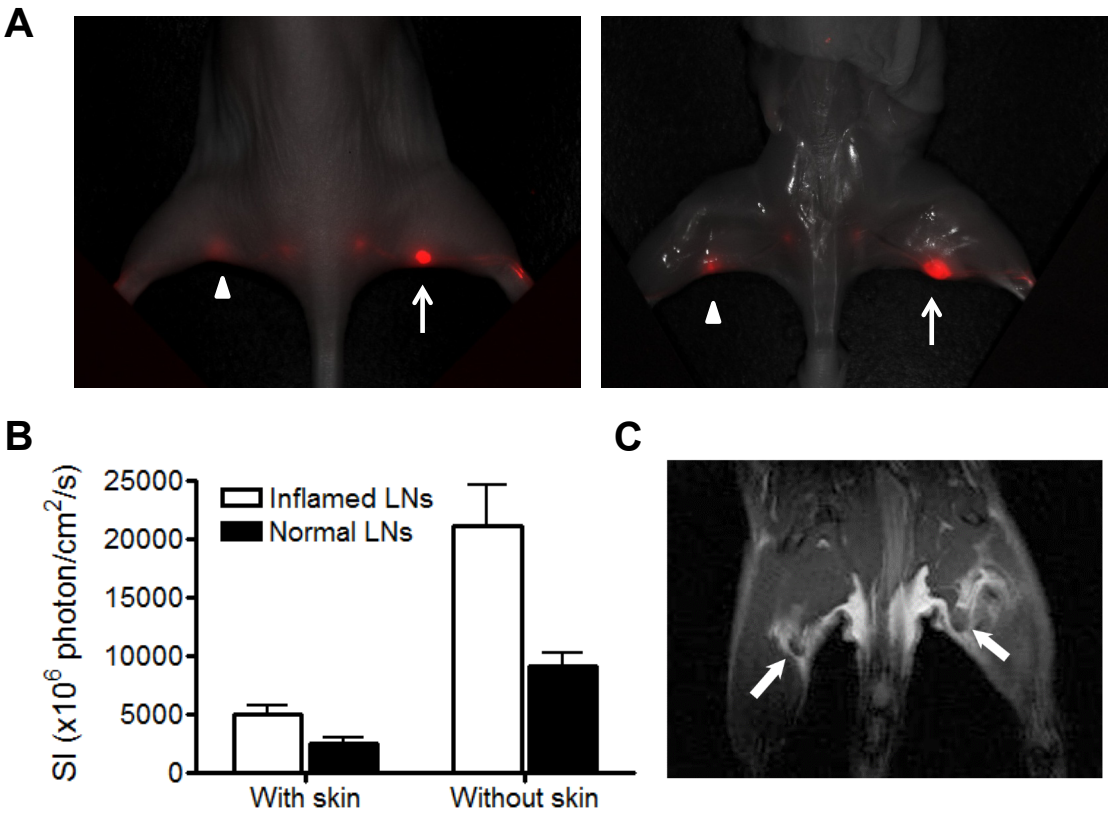

Supplemental Figure 2. Fluorescence imaging of inflamed lymph nodes with Cy5.5-HA10K. Inflammation was induced in BALB/c mice (n = 6) by intramuscular injection of turpentine oil (10 μL) (right hind leg). The mice were subjected to MRI and optical imaging on day 5 after injection according to previous reported time course of inflammatory responses (1, 2). MRI was performed on a high magnetic field micro-MR scanner (7.0 T, Bruker, Pharmascan) with small animal-specific body coil. Mice were maintained anesthetized by keeping inhaling isoflurane (1.5–2%) in O_2 and were kept warm by circulating warm water (37 °C). T_2-weighted images were acquired by a multislice multiecho (MSME) sequence and the parameters were as the following: repetition time (TR), 2,500 ms; effective echo time (TE), 45 ms; number of excitations (NEX), 1; matrix size, 256 × 256; field of view (FOV), 4 × 4 cm; slice thickness, 1 mm. For optical imaging, Cy5.5-HA10K (0.2 nmol of Cy5.5 in 20 μL) were injected into both sides of hock of mice. Optical imaging was performed 2 hrs after injection. (A) Representative fluorescence images of normal (left leg, white arrowhead) and inflamed (right leg, arrow) popliteal LN with (left) and without (right) skin. Strong fluorescence signal from Cy5.5-HA10K was observed in the inflamed popliteal LN. (B) Quantitative analysis of normal and inflamed popliteal fluorescence intensity. The signal intensity from the inflamed LNs is significantly higher than that from the control LNs ($P < 0.05$). (C) T_2-weighted MRI of popliteal LN (white arrows). Inflamed popliteal (right) LN is remarkably enlarged.

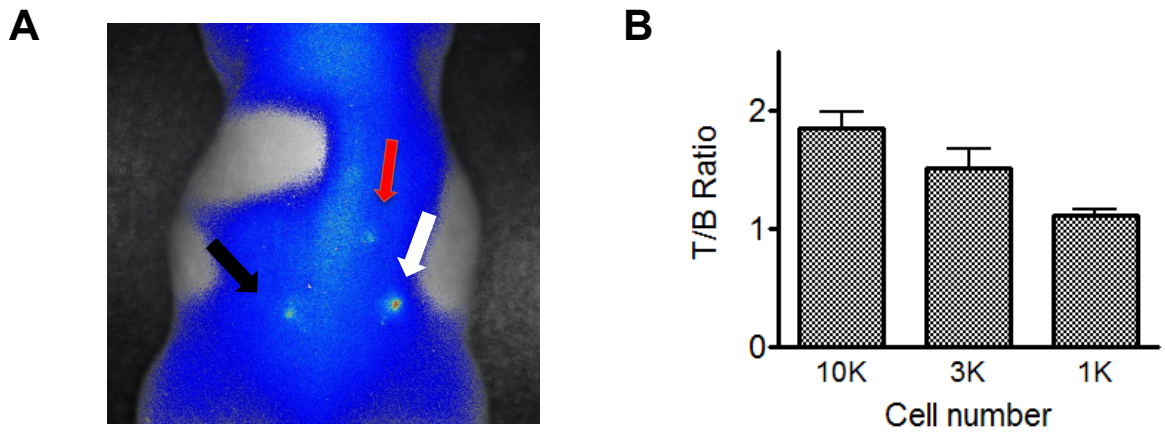

Supplemental Figure 3. Sensitivity of IRDye800-cetuximab in detecting UM-SCC-22B tumor cells in vivo. To evaluate the sensitivity of IRDye 800-cetuximab in detecting UM-SCC-22B tumor cells *in vivo*, the UM-SCC-22B cells were incubated with IRDye 800-cetuximab (5 μmol/L) for 24 hrs. Different amount of cells (1K, 3K, 10K) were subcutaneously inoculated into the back of the nude mice (n=6). Immediately after the inoculation, the optical imaging was performed. (A) Representative fluorescence optical image. Injection sites are indicated by arrows (white arrow, 10K cells; black arrow, 3K cells; red arrow, 1K cells). (B) Quantitative analysis of tumor cells to background ratios.

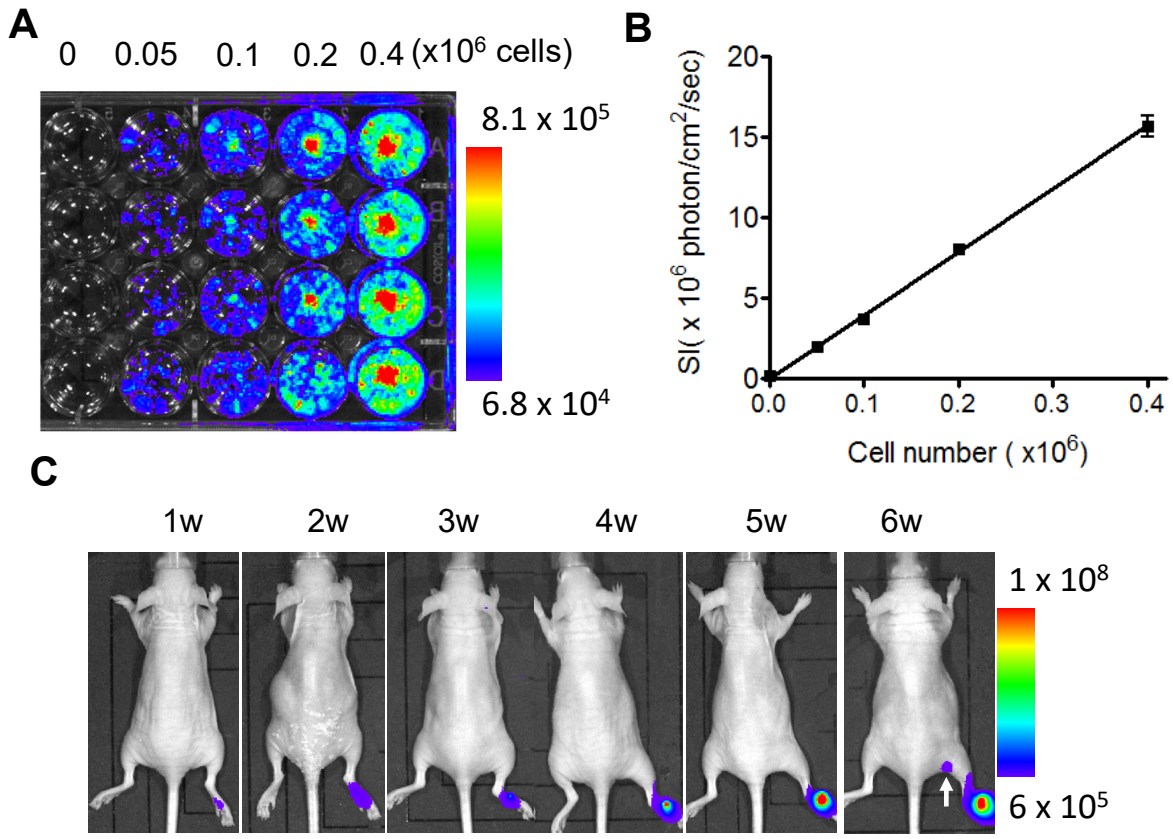

Supplemental Figure 4. Development and monitoring of UM-SCC-22B metastasis model. (A) Fluc$^+$ UM-SCC-22B cells were trypsinized and resuspended in DMEM medium. Then the cells were seeded in a 24-well plate with different concentration of cells per well. After 24 hours incubation, D-luciferin (5μL, 33 mg/mL, Sigma-Aldrich) was added to each well and the plate was scanned by using a Lumina II imaging system (Caliper Life Sciences). (B) Quantitative analysis of the bioluminescence signal intensity. There is a linear correlation between the signal intensity and cell number. (C) Representative longitudinal bioluminescent imaging of mice after hock injection of 0.1 x 10^6 Fluc$^+$ UM-SCC-22B cells. Imaging was performed once a week using a Lumina II imaging system (Caliper Life Sciences). Each time, 150 mg/kg D-luciferin in 100 μL of normal saline was administrated via intraperitoneal injection and mice were imaged 10 min after. Mice were kept anesthetized by 2% isoflurane during the imaging process. The tumor metastasis was pointed out by the white arrow.

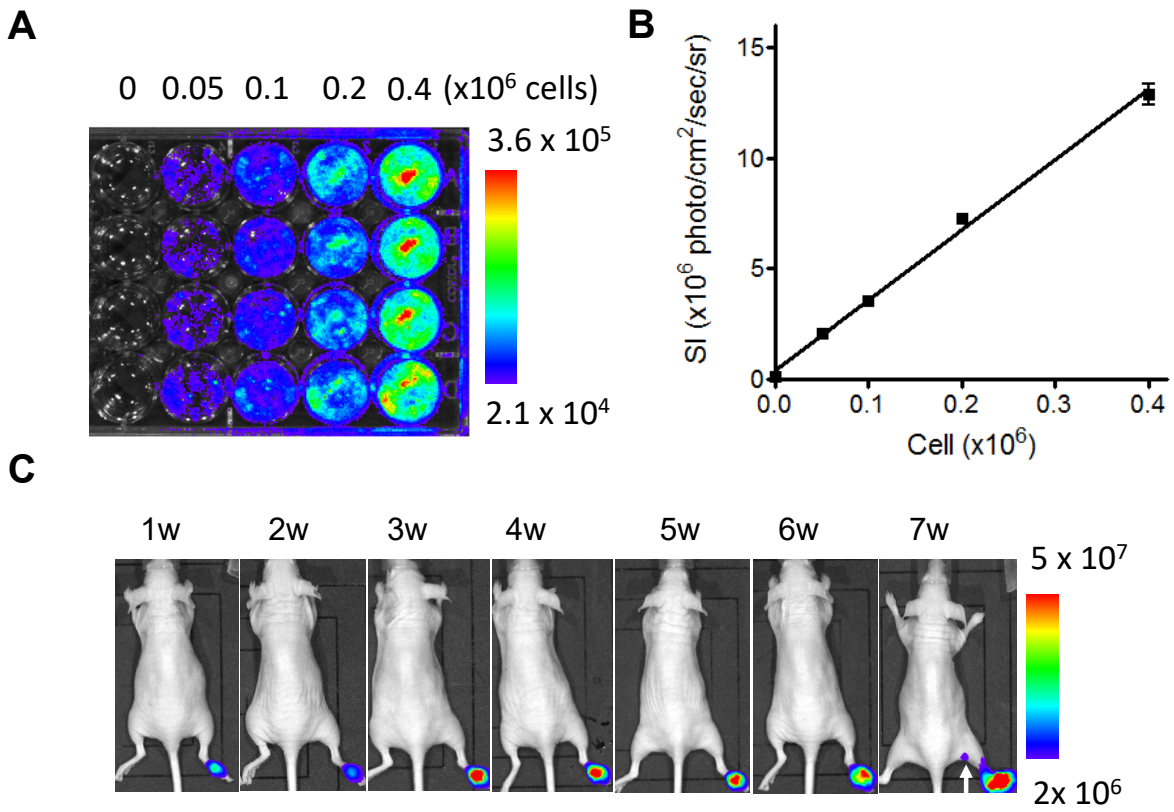

Supplemental Figure 5. Development and monitoring of SKOV-3 metastasis model. (A) Fluc$^+$ SKOV-3 cells were trypsinized and resuspended in DMEM medium. Then the cells were seeded in a 24-well plate with different concentration of cells per well. After 24 hours incubation, D-luciferin (5μL, 33 mg/mL, Sigma-Aldrich) was added to each well and the plate was scanned by using a Lumina II imaging system (Caliper Life Sciences). (B) Quantitative analysis of the bioluminescence signal intensity. There is a linear correlation between the signal intensity and cell number. (C) Representative longitudinal bioluminescent imaging of mice after hock injection of 0.1 x 10^6 Fluc$^+$ SKOV-3 cells. Imaging was performed once a week using a Lumina II imaging system (Caliper Life Sciences). Each time, 150 mg/kg D-luciferin in 100 μL of normal saline was administrated via intraperitoneal injection and mice were imaged 10 min after. Mice were kept anesthetized by 2% isoflurane during the imaging process. The tumor metastasis was pointed out by the white arrow.

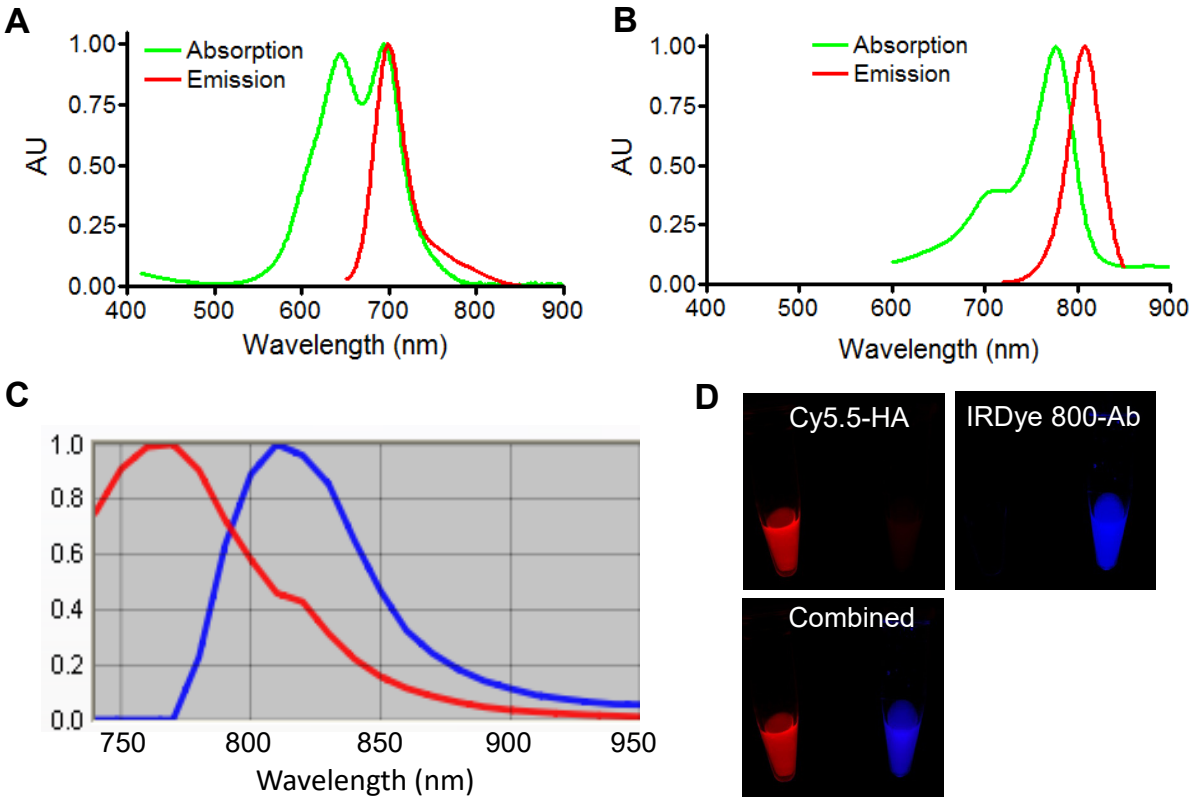

Supplemental Figure 6. Separation of fluorescence signals from Cy5.5-HA10 and IRDye800-mAb. Fluorescence spectra of Cy5.5- HA10K (A) and IRDye 800-cetuximab (B). (C) Emission spectra of Cy5.5-HA10K and IRDye800-cetuximab acquired by Maestro II optical imaging system using a NIR filter set (excitation 704 nm, emission 745 nm longpass). (D) Unmixed image of Cy5.5-HA10K and IRDye800-cetuximab using the spectra displayed in panel C.

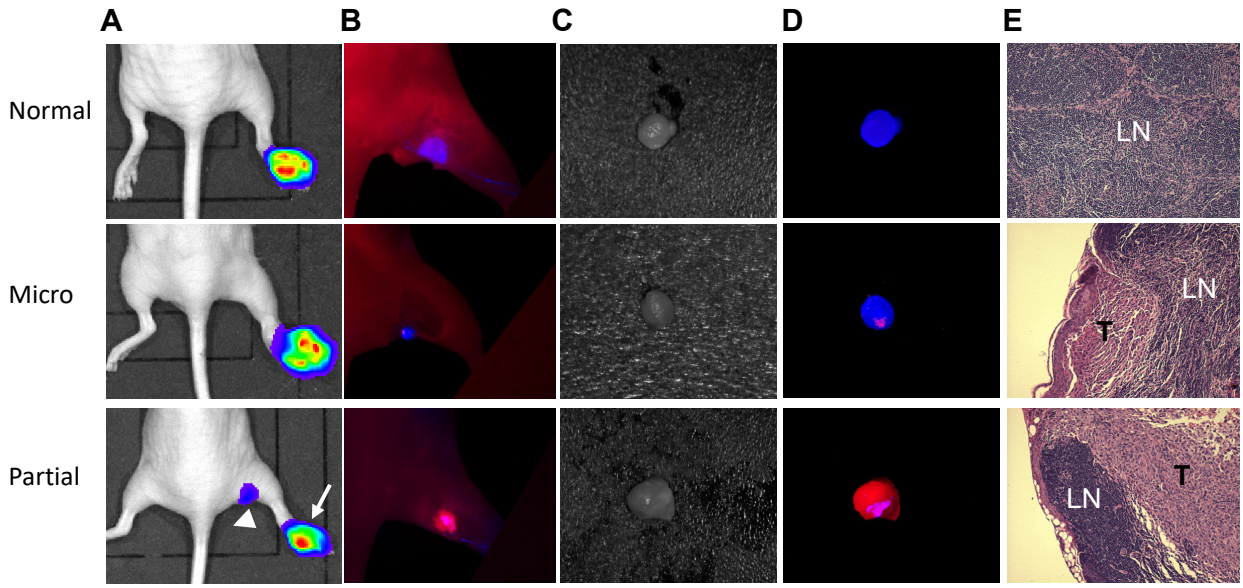

Supplemental Figure 7. Mapping tumor metastasis in sentinel lymph nodes by dual-probe fluorescence optical imaging in SKOV-3 metastasis model. (A) LN metastasis model was developed by hock injection of Fluc-SKOV-3 cells and the metastases were confirmed by BLI. The original tumor sites were pointed by arrows and tumor metastasized LNs by arrow heads. (B) IRDye800-Trastuzumab (anti-EGFR antibody) was injected intravenously at 24 h before imaging and Cy5.5-HA (10K) was administered locally at 2 h before imaging with a Maestro II optical imaging system. The fluorescence signal was unmixed based on the corresponding specific spectra from Cy5.5 (designated as red) and IRDye800 (designated as blue). The skin was peeled to mimic the operative environment. (C) Bright field and (D) optical imaging of excised LNs. LN without tumor invasion showed red color only from Cy5.5-HA (upper). Partially tumor invaded LN showed mixed signals from both Cy5.5-HA and IRDye800-Trastuzumab (lower). (E) H&E staining of corresponding LNs. T, tumor tissue; LN, lymphatic tissue.

References

1. Yamada S, Kubota K, Kubota R, Ido T, Tamahashi N. High accumulation of fluorine-18-fluorodeoxyglucose in turpentine-induced inflammatory tissue. J Nucl Med. 1995;36:1301-6.
2. Wu C, Yue X, Lang L, Kiesewetter DO, Li F, Zhu Z, et al. Longitudinal PET imaging of muscular inflammation using 18F-DPA-714 and 18F-Alfatide II and differentiation with tumors. Theranostics. 2014;4:546-55.